*SF2A 2013*
*L. Cambrésy, F. Martins, E. Nuss and A. Palacios (eds)*

# MASS ASSEMBLY IN QUIESCENT AND STAR-FORMING GALAXIES SINCE $Z \simeq 4$ FROM ULTRAVISTA DR1 IN THE COSMOS FIELD

O. Ilbert[1], H. J. McCracken[2], O. Le Fèvre[1], P. Capak [3], J. Dunlop [4], A. Karim [5], M. A. Renzini [6], K. Caputi[7], S. Boissier[1] and the COSMOS team

**Abstract.** We estimate the galaxy stellar mass function and stellar mass density for star-forming and quiescent galaxies out to $z = 4$. We construct a sample of 220000 galaxies selected at $K_s < 24$. Our analysis is based on photometric redshifts with a precision of $\sigma_{\Delta z/(1+z)} = 0.008$ at $i^+ < 22.5$ and $\sigma_{\Delta z/(1+z)} = 0.03$ at $1.5 < z < 4$. We find a mass-dependent evolution of the global and star-forming populations, with the low-mass end of the mass functions evolving more rapidly than the high-mass end. For the mass function of the quiescent galaxies, we do not find any significant evolution of the high-mass end at $z < 1$ while we observe a clear flattening of the faint-end slope. From $z \sim 3$ to $z \sim 1$, the mass density of quiescent galaxies increases by 1.6 dex. We investigate the link between direct SFRD measurements and the evolution of the mass density. The star formation history that we infer from our mass density evolution is in excellent agreement with direct SFRD measurements at $z < 1.5$, while we find differences of 0.2 dex at $z > 1.5$ consistent with the expected uncertainties. Finally, we present a new method to infer the specific star formation rate from the mass function of star-forming galaxies and we find a continous increase of the sSFR with redshift out to $z \sim 4$. The photometric catalogues and associated photometric redshifts are available at http : //terapix.iap.fr/article.php?id_article = 844.

Keywords: Galaxies: distances and redshifts – Galaxies: evolution – Galaxies: formation – Galaxies: star formation – Galaxies: stellar content

## 1 Introduction

The galaxy stellar mass function (hereafter MF) is a fundamental indicator of the physical processes that regulate mass assembly in galaxies across cosmic time. Stellar mass assembly in galaxies is the result of star formation and mergers. Star formation is regulated by numerous physical processes: the amount of accreted gas available by radiative cooling or cold accretion ; AGN feedback which could shut down the star formation ; or by other processes such as supernovae-driven winds in less massive haloes. The relative contribution and operating timescales of these different processes regulate the stellar mass growth and the migration from star-forming galaxies to quiescent galaxies. The evolutionary tracks of the quiescent and star-forming MF as a function of look-back time reveal the major paths taken by different galaxy populations across cosmic time. This measurement quantifies the efficiency in forming new stellar populations and the quenching efficiency depending on the epoch and galaxy mass.

Measuring the stellar masses is challenging beyond $z \sim 1$: the availability of deep wide field near-IR multi-band photometry is essential. Spectral features like the D4000 or Balmer break move into the near-IR at $z > 1.5$, and several near-IR bands are required to properly sample the spectral energy distribution (SED) and enable stable photometric redshifts and stellar masses from SED-fitting techniques. The COSMOS field is one of the best available fields to derive the MF thanks to the large area (2 deg$^2$) and the large amount of deep ($I_{AB} \sim 26.5$) multi-wavelength data available (more than 35 bands). The UltraVISTA survey covered 1.5 deg$^2$ of the COSMOS field with deep NIR data ($K_s < 24$). Thanks to these data, we were able to derive accurate photometric redshifts at $z > 1.5$, well tested with more than 35000 spectroscopic redshifts. We estimated the galaxy stellar mass function and stellar mass density for star-forming and quiescent galaxies out to $z = 4$. This study is published in Ilbert et al. (2013).

[1] Aix Marseille Université, CNRS, LAM (Laboratoire d'Astrophysique de Marseille) UMR 7326, 13388, Marseille, France
[2] Institut d'Astrophysique de Paris, UMR7095 CNRS, Université Pierre et Marie Curie, 98 bis Boulevard Arago, 75014 Paris, France
[3] Spitzer Science Center, California Institute of Technology, Pasadena, CA 91125, USA
[4] Institute for Astronomy, University of Edinburgh, Royal Observatory, Edinburgh, EH9 3HJ, UK
[5] Argelander-Institute of Astronomy, Bonn University, Auf dem Hügel 71, D-53121 Bonn, Germany
[6] Dipartimento di Astronomia, Universita di Padova, vicolo dell'Osservatorio 2, I-35122 Padua, Italy
[7] Kapteyn Astronomical Institute, University of Groningen, P.O. Box 800, 9700 AV Groningen, the Netherlands

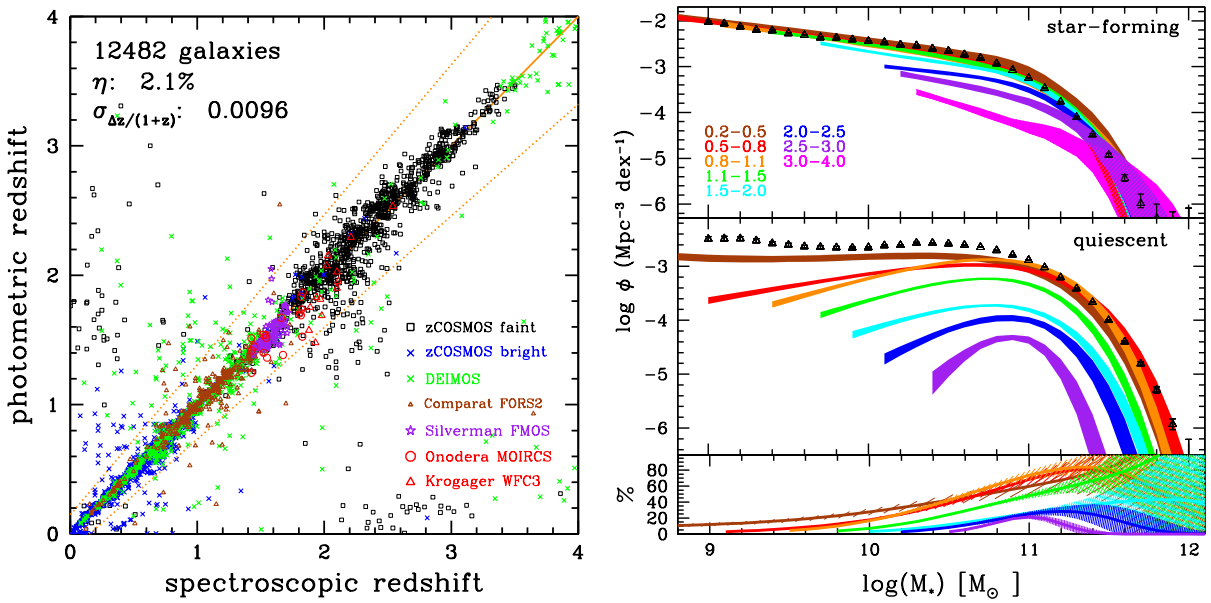


**Fig. 1. Left:** Photometric redshifts versus spectroscopic redshifts. Only secure spectroscopic redshifts at $K_s < 24$ are considered. Different colors color to the different spectroscopic samples listed in section 2. **Right:** Galaxy stellar mass functions up to $z = 4$ for the star-forming population (top panel) and for the quiescent population (middle panel). The fraction of quiescent is given in the bottom panel. Each color corresponds to a redshift bin.

## 2 Data

Our photometric catalogue comprises near-infrared data taken on the VISTA telescope as part of the UltraVISTA project and optical broad and intermediate-band data taken with the SUPRIME camera on Subaru in support of the COSMOS project (Capak et al. 2007). The near-infrared data we use here corresponds to the UltraVISTA DR1 data release fully described in McCracken et al. (2012). The first UltraVISTA DR1 data release covers 1.5 deg$^2$ in four near-infrared filters $Y$, $J$, $H$ and $K_s$. Fluxes are measured on PSF-homogenised images in 25 bands including optical broad and intermediate-band Subaru data taken for the COSMOS project. We also add four bands at $3.6-8\mu m$ from S-COSMOS and the GALEX NUV band. We keep only the sources at $K_s < 24$ located in areas with a good image quality.

The photometric redshifts are derived using `Le_Phare` (Arnouts et al. 2002, Ilbert et al. 2006) following a procedure similar to Ilbert et al. (2009). We use elliptical and spiral galaxy templates from the Polletta et al. (2006) library, complemented with blue star-forming templates generated with Bruzual & Charlot (2003) SPS models. Extinction is added as a free parameter and several extinction laws are considered (Calzetti et al. 2000, Prevot 1984 and a modified version of the Calzetti laws including a bump at 2175Å). Emission lines are added to the templates using an empirical relation between the UV light and the emission line fluxes.

It is essential to check that our photo-z are robust at $z > 1.5$ before extending our analysis at higher redshift. We combine several spectroscopic samples to test the accuracy of the photometric redshifts, including zCOSMOS-bright with 20700 bright VIMOS/VLT spectra selected at $i^+ < 22.5$ (Lilly et al. 2007), zCOSMOS faint with 9500 faint VIMOS/VLT spectra selected at $1.5 < z < 3$ (Lilly et al., in preparation), 2300 DEIMOS/Keck redshifts which combined several selected sub-populations of blue star-forming and infrared galaxies at $0.5 < z < 6$ (Capak et al., in preparation), 835 FORS2/VLT redshifts at $0.6 < z < 1.8$ (Comparat et al., in preparation), 138 FMOS/Subaru redshifts at $1.4 < z < 1.8$ (Silverman et al., in preparation), 18 faint quiescent galaxies at $z < 1.9$ obtained with MOIRCS/Subaru (Onodera et al. 2012) and 16 faint quiescent galaxies at $1.85 < z < 2.6$ obtained with the WFC3 grism observations from the 3D-HST survey (Krogager et al., 2013).

The comparison between photometric and spectroscopic redshifts is shown in Figure.1. Our photometric redshifts have two regimes: at $i^+_{AB} < 22.5$ ($z_{med} \sim 0.5$), precision 1% with less than 1% of catastrophic failures. In the high redshift range $1.5 < z < 4$, the precision of the photo-z is tested against the zCOSMOS faint sample, and is 3% for $i^+_{med} \sim 24$ galaxies. Therefore, we can ensure that our photo-z are robust at $z > 1$ and we are now able to extend MF measurements to $z = 4$.

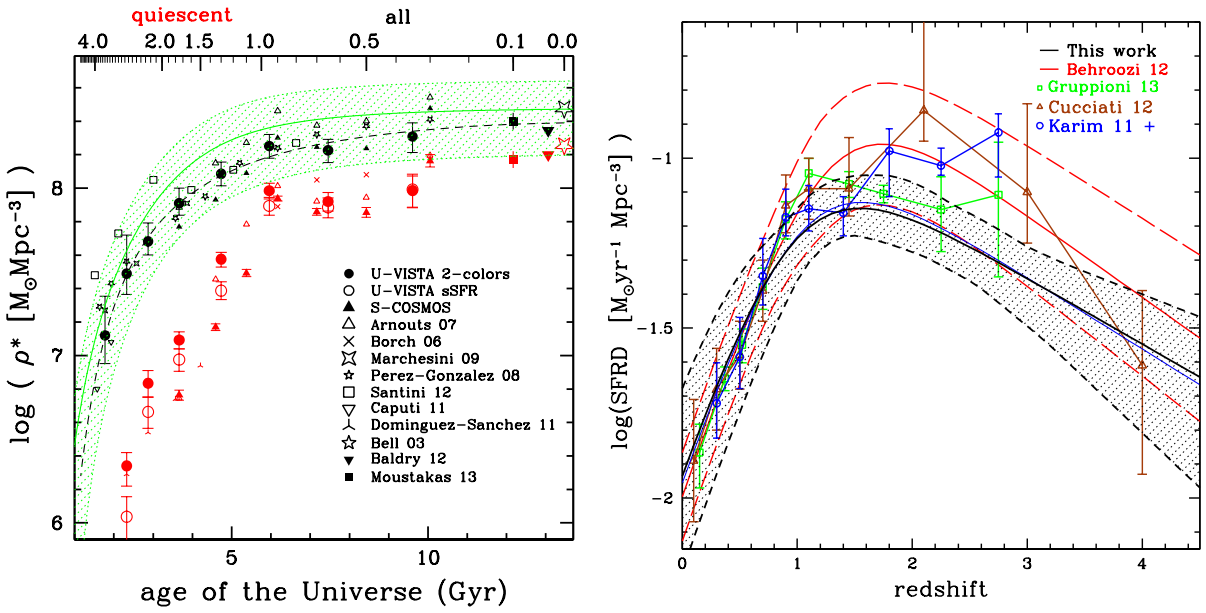


**Fig. 2. Left:** Stellar mass density as a function of cosmic time. Black and red points correspond to the full and quiescent populations, respectively. The solid circles correspond to our new results using UltraVISTA. The green shaded area corresponds to the cosmic SFR compiled by Behroozi et al. (2013) and integrated over cosmic time. **Right:** A comparison between the star formation history inferred from the UltraVISTA mass density (black solid line and dashed area) and direct SFRD measurements listed in Section 3.

## 3 Evolution of the Stellar Mass Function and Mass Density

We used stellar population synthesis (SPS) models to convert luminosity into stellar mass. The templates are generated using the SPS models from Bruzual & Charlot (2003), assuming exponentially declining star formation histories. We measured the stellar mass functions using the tool ALF (Ilbert et al. 2005). This tool includes several non-parametric estimators and we verified that the three non-parametric estimators are in good agreement over the considered mass ranges (Ilbert et al. 2004). Our error budget includes the Poissonian errors, the photo-z and stellar mass uncertainties and the cosmic variance. We also correct for the Eddington bias when we fit the non-parametric data.

Right panel of Figure 1 shows the MFs of quiescent and star-forming galaxies. We isolate the quiescent population using a classification based on the rest-frame colours $NUV - r^+$ and $r^+ - J$. This classification separates cleanly dusty star-forming galaxies and quiescent galaxies. We do not find any significant evolution of the high-mass end at $z < 1$ for the quiescent population (any evolution being limited to $\Delta M < 0.2dex$), while we observe a clear flattening of the slope in the same redshift range. We interpret this evolution of the low-mass end of the MF as arising from continuous quenching of galaxies between $z \sim 1$ and $z \sim 0.1$, probably by physical processes related to environment (see Peng et al. 2010).

The UltraVISTA data allow us to trace the growth in stellar mass density in quiescent galaxies from $z \sim 3$ to the present day. From $z \sim 3$ to $z \sim 1$ we find a rapid increase in the stellar mass density of all quiescent galaxies, independent of stellar mass. We confirm that the steep rise of more than one order of magnitude of this population between $1 < z < 2$ observed in previous works (Arnouts et al., 2007; Ilbert et al., 2010). This must indicate that a fraction of star-forming galaxies is continuously quenched at $z > 1$. Because of the different faint-end slopes of the MF between the quiescent and global populations at $z < 3$, we infer that the physical processes which quench the star formation are more efficient above $\mathcal{M} \gtrsim 10^{10.7-10.9}\mathcal{M}_{\odot}$. This scenario is consistent with the model proposed by Peng et al. (2010) who introduce a "mass quenching" process. Since the high-mass end of the quiescent MF stops evolving at $z < 1$, we conclude that: 1) star formation is not efficient enough at $z < 1$ to produce new massive star-forming galaxies, which could be quenched later; 2) major mergers between massive galaxies are not sufficiently frequent at $z < 1$ to increase significantly the density of massive quiescent galaxies.

We find that the evolution of the star-forming MF is strongly mass-dependent. The low-mass end evolves more rapidly than the high-mass end. If we consider an evolution purely driven by star formation, the low-mass galaxies evolve by almost 1 dex between $1.5 < z < 2$ and $0.2 < z < 0.5$, while the stellar mass of the most massive galaxies increases by less than 0.2 dex in the same time interval. The lack of evolution of the massive end can be interpreted as a direct consequence of star formation being drastically reduced or quenched when a galaxy becomes more massive than $\mathcal{M} > 10^{10.7-10.9}\mathcal{M}_{\odot}$.

## 4 Link the star formation history and mass density

In Figure 2 (left), we compare the mass density obtained with our data (solid black circles) and the mass density evolution expected by integrating the SFRD compilation of Behroozi et al. (2013, green line and shaded area). We find that the expected mass density is systematically higher by 0.05-0.2 dex than our data, while still consistent with the uncertainties.

We also infer the star formation history from the mass density evolution following Wilkins et al. (2008). We parametrize the star formation history with three free parameters. We fit these three free parameters to reproduce the observed mass density. Our inferred star formation history and the associated uncertainties are shown with the black solid line and the shaded area in Figure 2 (right). The inferred star formation history is compared with the data compiled by Behroozi et al. (2013) and the most recent measurements of the SFRD at $0 < z < 4$ based on UV (Cucciati et al. 2012), IR (Gruppioni et al. 2013) and radio data (Karim et al. 2011). This inferred star formation history is in excellent agreement with SFRD measurements at $z < 1.5$, while we find differences of 0.2 dex at $z > 1.5$. However, considering the size of the uncertainties at $z > 1.5$, the SFRD and mass density data still provide a consistent picture of the star formation history.

We also develop a new method to estimate the specific SFR (SFR/M) from the mass function evolution. By comparing the star-forming MFs at two different epochs (after having removed the contribution of galaxies quenched during the considered time interval), we derive the sSFR from $z \sim 0.5$ up to $z < 4$. We find that the sSFR increases continuously at $1 < z < 4$ for our considered mass range $10^{10}\mathcal{M}_{\odot} \leq \mathcal{M} \leq 10^{10.5}\mathcal{M}_{\odot}$. This new method is complementary to direct sSFR measurements at $z > 2$, which are very sensitive to dust extinction (e.g. Bouwens et al. 2009) or SED modeling (e.g. Stark et al. 2013).

We gratefully acknowledge the contributions of the entire COSMOS collaboration consisting of more than 100 scientists. More information on the COSMOS survey is available at http://www.astro.caltech.edu/cosmos. Based on data products from observations made with ESO Telescopes at the La Silla Paranal Observatory under ESO programme ID 179.A-2005 and on data products produced by TERAPIX and the Cambridge Astronomy Survey Unit on behalf of the UltraVISTA consortium.

## References

Arnouts S., Moscardini L., Vanzella E. et al., 2002, MNRAS, 329, 355
Arnouts S., Walcher C.J., Le Fèvre O. et al., 2007, A&A, 476, 137
Behroozi P.S., Wechsler R.H. & Conroy C., 2013, 770, 57
Bruzual G. & Charlot S., 2003, MNRAS, 344, 1000
Calzetti D., Armus L., Bohlin R.C. et al., 2000, ApJ, 533, 682
Capak P., Abraham R.G., Ellis R.S. et al., 2007, ApJS, 172, 284
Cucciati O., De Lucia G., Zucca E. et al., 2012, A&A, 548, 108
Eddington A. S., 1913, MNRAS, 73, 359
Gruppioni C., Pozzi F., Rodighiero G. et al., 2013, MNRAS, 432, 23
Ilbert O., Tresse L., Arnouts S. et al., 2004, MNRAS, 351, 541
Ilbert O., Tresse L., Zucca E. et al., 2005, A&A, 439, 863
Ilbert O., Arnouts S., McCracken H.J. et al., 2006, A&A, 457, 841
Ilbert O., Capak P., Salvato M. et al., 2009, ApJ, 690, 1236
Ilbert O., Salvato M., Le Floc'h E. et al., 2010, ApJ, 709, 644
Ilbert O., McCracken H.J., Le Fèvre O. et al., 2013, A&A, 556, A55
Karim A., Schinnerer E., Martínez-Sansigre A. et al., 2011, ApJ, 730, 61
Krogager J.K et al., 2013, submitted to ApJ, astro-ph/1309.6316
Lilly S.J., Le Fèvre O., Renzini A. et al., 2007, ApJS, 172, 70
McCracken H.J., Milvang-Jensen B., Dunlop J. et al., 2012, A&A, 544, 156
Onodera M., Renzini A., Carollo M. et al., 2012, ApJ, 755, 26
Peng Y.J., Lilly S.J., Kovač K. et al., 2010, ApJ, 721, 193
Polletta M., Tajer M., Maraschi L. et al., 2007, ApJ, 663, 81
Scoville N., Aussel H., Brusa M. et al. 2007, ApJS, 172, 1
Stark D., Schenker M.A., Ellis R. et al., 2013, ApJ, 763, 129
Wilkins S.M., Trentham N. & Hopkins A.M., 2008, MNRAS, 385, 687